

## Molecular Aggregation in Poly(vinyl Chloride)

A. H. ABDEL-ALIM and A. E. HAMIELEC,  
*Department of Chemical Engineering,  
 McMaster University, Hamilton, Ontario, Canada*

### Synopsis

Molecular weight distributions and molecular aggregation for poly(vinyl chloride) (PVC) polymerized in bulk at  $-10$ ,  $-30$ , and  $-50^{\circ}\text{C}$  have been measured using gel permeation chromatography. The aggregate content in PVC polymerized at  $-50^{\circ}\text{C}$  was found to be 87 wt-%. These spherical aggregates of mean diameter of 5000 Å are formed preferentially from PVC chains having high molecular weights and long syndiotactic sequence lengths. A temperature of  $200^{\circ}\text{C}$  was used to disintegrate these aggregates into single PVC molecules. In disagreement with measurements of  $\bar{M}_n$  and  $\bar{M}_w$  published in the literature, our measured values do not reach a minimum but rather increase continuously with decreasing temperature of polymerization. This disagreement is most probably due to the phenomenon of molecular aggregation in PVC.

### INTRODUCTION

It has been known for some time that PVC molecules form aggregates and that these supermolecular entities dissolve very slowly in good solvents such as THF and cyclohexanone. The discovery of PVC aggregates dates back to the early work of Doty.<sup>1</sup> More recently, workers have become aware of the need to disintegrate these aggregates into single PVC molecules to preclude anomalous molecular weight measurements.<sup>2,3,4</sup> Lyn-gaae-Jorgensen<sup>5</sup> did rheological measurements on PVC melts containing aggregates and found that flow properties were significantly affected. He employed light-scattering techniques and estimated the aggregates to have the shape of a star-branched polymer with approximately 24 long branches of random length held together in a crystalline nucleus. In an earlier investigation,<sup>4</sup> we developed a quantitative method based on gel permeation chromatography for the measurement of wt-% aggregates and size distribution of aggregates in a PVC sample. The present investigation is an extension of this earlier study and considers aggregates in PVC polymerized in bulk at temperatures as low as  $-50^{\circ}\text{C}$ . In addition, the molecular weight distribution and syndiotacticity (NMR) of these PVC samples were measured.

## EXPERIMENTAL

### Materials

Low-temperature PVC samples were polymerized in bulk using  $\gamma$ -ray initiation at  $-10^{\circ}\text{C}$ ,  $-30^{\circ}\text{C}$ , and  $-50^{\circ}\text{C}$  and were supplied for this investigation by G. Palma, Laboratorio di Fotochimica e Radiazioni d'Alta Energia C.N.R., Padova, Italy. Initiation involved a dose rate of 2.2 rad/sec, giving conversions in the range of 78% to 90%.

The remaining PVC samples were polymerized in bulk using chemical initiation (AIBN). Details of these samples are available in an earlier paper.<sup>4</sup>

### GPC Measurements

A Waters GPC Model 200 was used; THF ( $25^{\circ}\text{C}$ ) was the solvent; Polymer concentration was 0.2 wt-%; flow rate, 3 ml/min. Nine columns in series of the following specifications were used: Bio-glass, 2500/1500 Å; CPG 10-2000/1250 Å; CPG 10-2000/1250 Å; Styragel,  $5 \times 10^6$  Å; CPG 10-700 Å; Styragel,  $10^4$  Å; Styragel, 800 Å; Styragel, 350/100 Å; Styragel, 350/100 Å.

### NMR Measurements

Measurements were done at the Ontario Research Foundation by Dr. Arthur Grey of the NMR Center. A 220 MHz NMR with HMDS as internal reference and *o*-dichlorobenzene as solvent was used. Areas of peaks were measured by actual count and the triangular method; both agreed within 2% on the average.

## RESULTS AND DISCUSSION

Figure 1 is a flow diagram of the experimental procedure followed in this work. PVC solutions, 0.2 wt-% in THF, were prepared by mixing the appropriate amounts of polymer and THF. Dissolution was first tried at room temperature. At this stage, different polymer samples showed different solubility behavior. As mentioned in our previous paper,<sup>4</sup> PVC prepared at  $30^{\circ}\text{C}$  and above readily dissolved in THF at room temperature after stirring for about 1 hr or even less, giving a clear solution of single molecules and aggregates. On the other hand, the low-temperature PVC (polymerization temperature  $-10^{\circ}\text{C}$  and lower) did not give a clear solution at room temperature even with stirring for several days. The fraction of the polymer that remained in suspension was observed visually to be greater for the  $-50^{\circ}\text{C}$  and  $-30^{\circ}\text{C}$  PVC samples. Concentrations other than 0.2 wt-% were then tried to check whether concentration has any effect on the fraction in suspension. The results were the same, indicating that there is no concentration effect. This is expected, as we are far below the saturation limit.

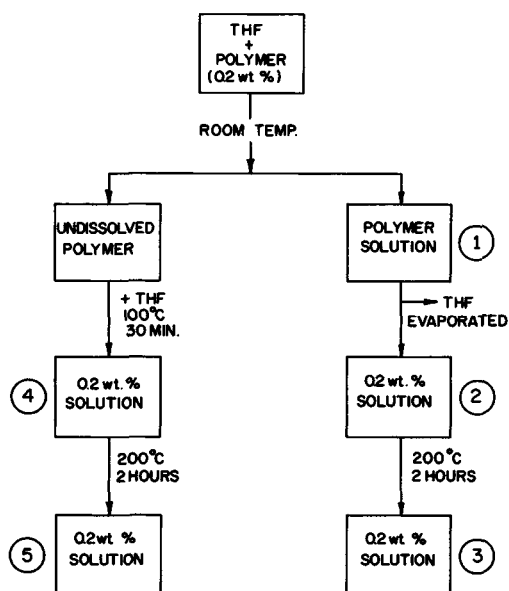


Fig. 1. Flow diagram of experimental procedure.

The fraction of polymer that remained in suspension was measured in two ways, first by filtering, washing, drying, and then weighing this material; and second by injecting the solution (the filtrate) in GPC and calculating the area of the chromatogram which is proportional to the concentration of this solution and then comparing this area to the area corresponding to standard PVC solutions of 0.2 wt-% concentration. Results of the two methods agreed within experimental error. This first injection is called injection 1, as shown in Figure 1. Following this, the undissolved polymer was mixed with calculated amounts of THF to make 0.2 wt-% solutions. This time, dissolution was done by heating the mixture at 100°C for 30 min under vacuum. This was found to be sufficient to dissolve the polymer. (It should be mentioned here that the word dissolution does not imply making a true solution on the molecular scale. All it means is producing a clear solution free of suspended matters.) This solution was then injected in GPC, and this was called injection 4. The solubility behavior of this fraction indicated that it was made of PVC aggregates due to molecular association of single molecules. This concept was proved to be true when these solutions (injection 4) were heated under vacuum for 2 hr at 200°C and then reinjected into the GPC (injection 5). This resulted in a different chromatogram shifted to the lower molecular weight side. Further heating did not result in further change. Heating at 150°C for 2 hr did not cause disintegration of the aggregates. This was also observed by other workers.<sup>4,5,6</sup>

Going back to the first solutions (injection 1) knowing the concentrations of these solutions, calculated amounts of THF were evaporated to adjust

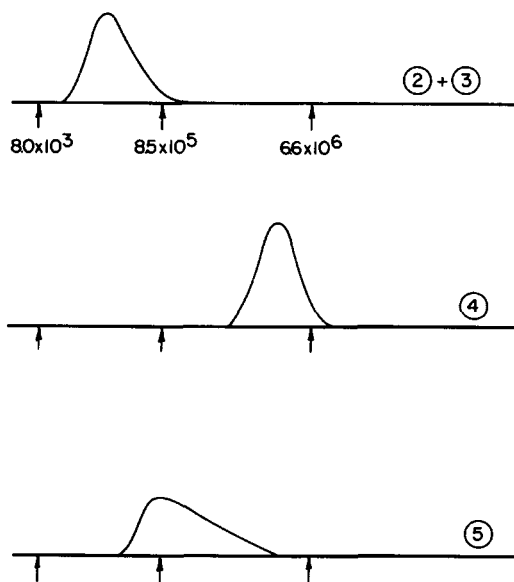


Fig. 2. GPC traces for  $-50^\circ\text{C}$  PVC. Numbers in circles refer to injection numbers as in Fig. 1.

the concentration to 0.2 wt-% (for easy comparison of areas). Injections of these solutions were called injections 2. As we did in our earlier study,<sup>4</sup> these solutions were heated to disintegrate aggregates. Injections after heat treatment were called injection 3. It is worth mentioning here that heating of PVC solutions was performed in glass ampoules of 10 mm O.D. and 8 mm I.D., under vacuum. No degradation products (HCl or green coloration) were noticed upon heating.

GPC results are given in Figure 2 for the  $-50^\circ\text{C}$  PVC. The arrows on the baseline indicate the molecular weight based on the molecular weight calibration curve of single PVC molecules. We noticed that injections 2 and 3 are identical. This indicates that all of the aggregates were in suspension and were filtered from the solution of single molecules at room temperature. PVC polymerized at  $-50^\circ\text{C}$  contains aggregates which do not dissolve in THF at room temperature. Comparison of injections 4 and 5 shows that the aggregates disintegrate on heating at  $200^\circ\text{C}$ . The distribution of injection 5 indicates that these aggregates are made up preferentially of the longer molecules of the original polymer.

Figure 3 shows GPC results for the  $-30^\circ\text{C}$  PVC. The size distribution of the aggregates and the molecular weight distribution of the single PVC molecules derived therefrom for the  $-50^\circ\text{C}$  and  $-30^\circ\text{C}$  PVC samples are identical. The wt-% aggregates at  $-50^\circ\text{C}$  is larger, however. In Figure 4, GPC results for the  $-10^\circ\text{C}$  PVC show a different type of behavior. Injections 2 and 3 are not the same, indicating that some of the aggregates in this polymer dissolve (but not disintegrate) at room temperature. Actually, these soluble aggregates disintegrated readily on heating

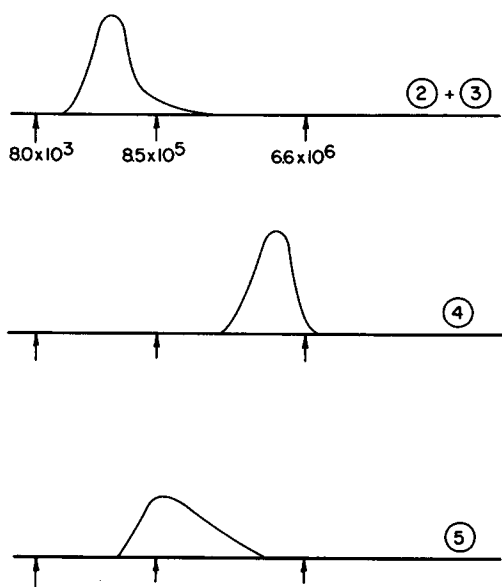


Fig. 3. GPC traces for  $-30^{\circ}\text{C}$  PVC. Numbers in circles refer to injection numbers as in Fig. 1.

at  $90^{\circ}\text{C}$  for 15 min; continuous heating at  $200^{\circ}\text{C}$  did not introduce further disintegration. The hatched area in Figure 4 is a measure of the amount of these aggregates.<sup>4</sup> However, some of the aggregates in the  $-10^{\circ}\text{C}$  PVC did not dissolve at room temperature, and they showed similar behavior to the aggregates in the  $-30^{\circ}\text{C}$  and  $-50^{\circ}\text{C}$  PVC. In our earlier study,<sup>4</sup> we noticed that aggregates present in PVC (polymerized at  $30\text{--}70^{\circ}\text{C}$ ) dissolved completely at room temperature, giving clear solutions.

From the above observations it appears that there are two kinds of aggregates formed in PVC. At very low polymerization temperatures, the aggregates are characterized by being insoluble in THF at room temperature, very stable toward heating. Severe heating is needed to disintegrate them into single molecules, and these aggregates are generally of large size, about  $4300\text{ \AA}$  in diameter (see Appendix), and are made up of the longer molecules of the original polymer. Accordingly, we shall call this kind a strong aggregate.

As polymerization temperature increases, another kind of aggregate—weak aggregate—starts to form. This kind dissolves readily in THF at room temperature. It disintegrates into single molecules by heating at lower temperatures. These aggregates are smaller in size, about  $2500\text{ \AA}$  in diameter (see Appendix), and they are made up of molecules of different molecular weights covering essentially the whole distribution of the original polymer.

In Table I we list the per cent aggregates measured for the different PVC samples; results from our previous work<sup>4</sup> are included. The second column in the table is the per cent of the strong aggregates. Weak aggre-

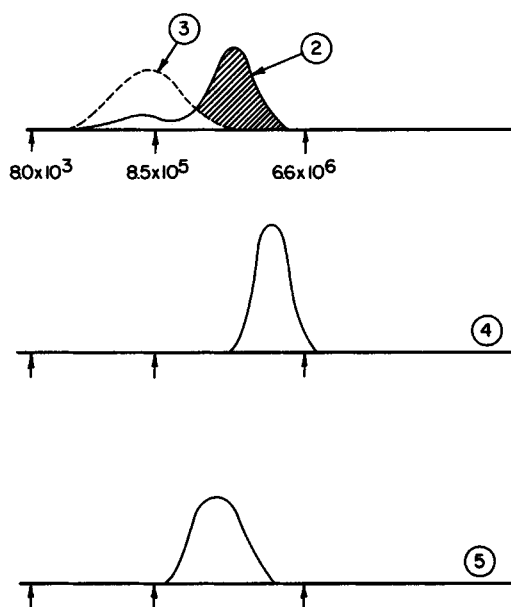


Fig. 4. GPC traces for  $-10^{\circ}\text{C}$  PVC. Numbers in circles refer to injection numbers as in Fig. 1.

gates are shown in the third column, and their sum, the total aggregate content, is given in the fourth column. The table also shows the tacticity results as measured by NMR.

The fractional total aggregate content (A) and the syndiotacticity (S) are plotted in an Arrhenius plot<sup>2</sup> in Figures 5 and 6, respectively. Figure 6 enables one to calculate the differences in enthalpy and entropy of activation for isotactic and syndiotactic monomer placements. Values obtained did not differ significantly from those we measured in our previous investigation.<sup>4</sup> Figure 5 shows an interesting feature. At higher poly-

TABLE I  
Aggregate Content and Tacticity of PVC Made at Different Temperatures

Polymerization temp., $^{\circ}\text{C}$	Undissolved polymer (strong), %	Aggregates by GPC (weak), %	Total aggregate, %	Syndiotacticity, %
70	—	—	—	54.4
50	—	—	—	55.9
45	—	1.2	1.2	56.5
40	—	2.5	2.5	56.8
37	—	3.9	3.9	57.0
30	—	10.9	10.9	57.6
-10	14.2	64.3	78.5	61.5
-30	82.8	—	82.8	64.7
-50	87.1	—	87.1	67.3

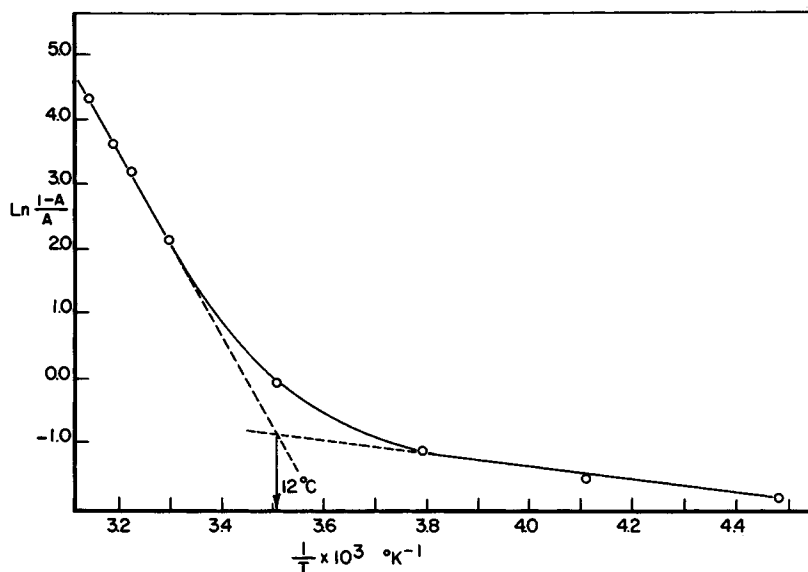


Fig. 5. Arrhenius plot of aggregate fraction (A) vs. absolute temperature of polymerization.

merization temperatures, a straight line is approached, with a slope of  $-1.48 \times 10^4$ , indicating that the amount of weak aggregates is very sensitive to polymerization temperature. At lower temperatures, a second straight line is approached, with a slope of  $-9.3 \times 10^2$ , indicating that aggregate content increases slowly with falling polymerization temperature.

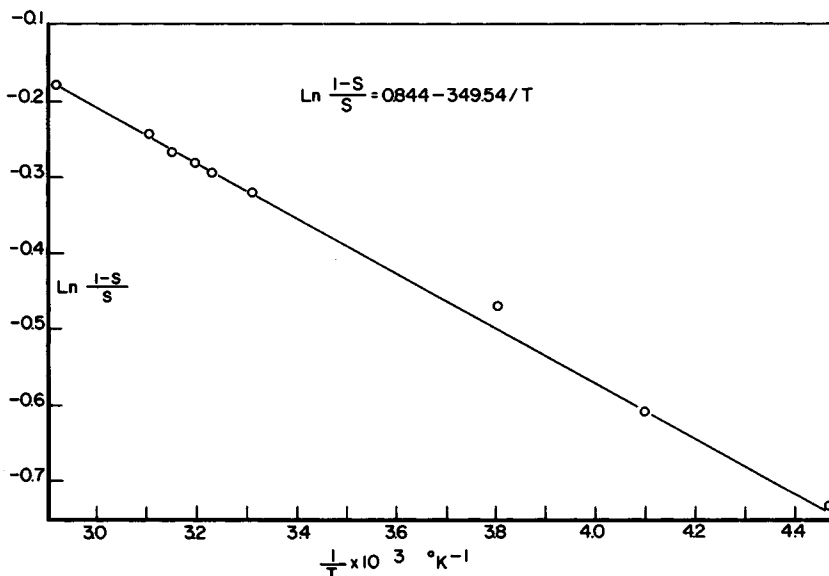


Fig. 6. Arrhenius plot of syndiotactic fraction (S) vs. absolute temperature of polymerization.

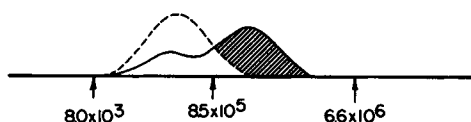


Fig. 7. GPC trace of the 12°C PVC: (—) before heating; (---) after heating.

The extensions of the two lines in Figure 5 intersect at a temperature of about 12°C. We then prepared a PVC sample at this temperature (using AIBN), and this PVC had only weak aggregates, as shown in Figure 7. The fraction of aggregates at this temperature was measured to be 0.55, and they were all of the weak type. This point was plotted on Figure 5 and lies in the transition region of the two types of behavior.

Data from Table I are plotted in Figure 8 to show how the wt-% of each type of aggregate and the total aggregate content varies with polymerization temperature. One can clearly see that for PVC prepared at very low temperatures ( $-50^{\circ}$  and  $-30^{\circ}\text{C}$ ), aggregates are insoluble in THF at room temperature.

Dotted lines are used to emphasize the uncertainty in estimation of critical temperatures for the formation of weak and strong aggregates. It

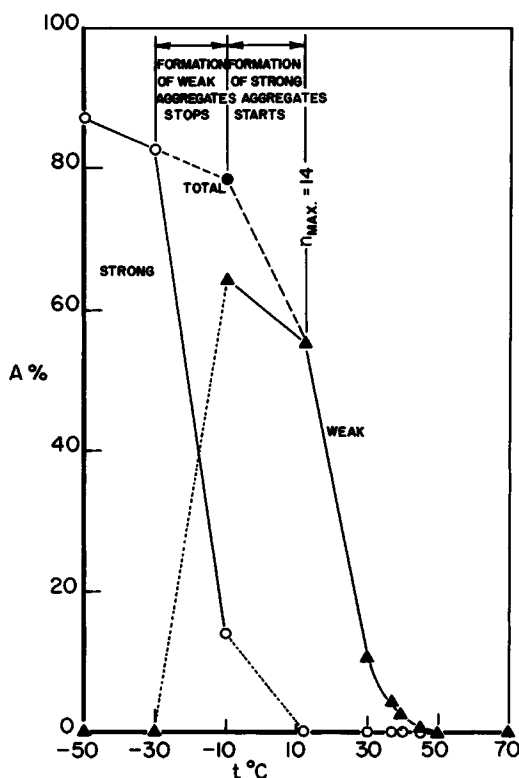


Fig. 8. Variation of per cent weak, strong, and total aggregates with polymerization temperature.



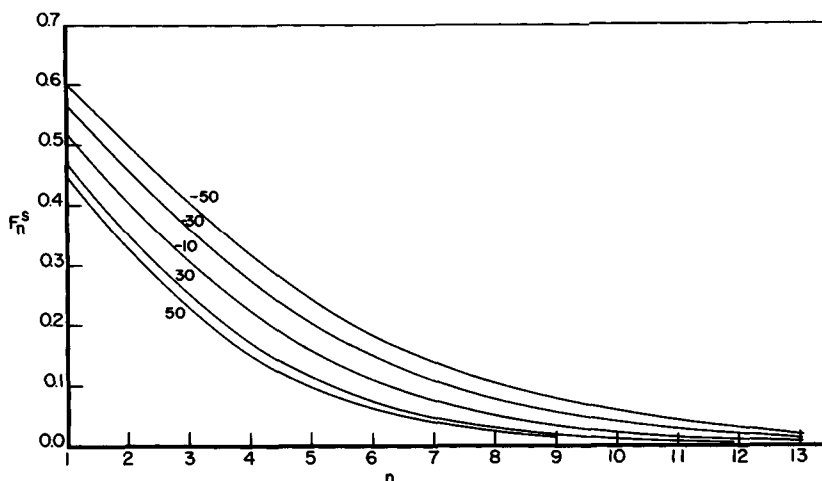


Fig. 9. Effect of polymerization temperature on the weight fraction of syndiotactic sequences ( $F_n^s$ ) of length greater than  $n$  monomer units.

is interesting to speculate on the reasons for the formation of two kinds of aggregates. Undoubtedly, syndiotacticity (sequence length distribution) and molecular weight of PVC play important roles in the formation of aggregates. It is well known that syndiotactic placements in PVC lead to crystallinity and aggregation.<sup>9</sup> The mere increase in the syndiotactic fraction with decreasing polymerization temperature does not fully explain the transition shown in Figure 5. The syndiotactic sequence length distribution most probably is in part responsible for the formation of strong aggregates. At lower temperatures of polymerization, relatively long syndiotactic sequences are formed. In Figure 9, the fraction ( $F_n^s$ ) of syndiotactic sequences of length greater than  $n$  is plotted versus sequence length  $n$  ( $n$  monomer units) for a range of polymerization temperatures. This fraction is given by

$$F_n^s = S^{n+1}(1 + (1 - S)n)$$

where  $S$  is the syndiotactic fraction. We calculated  $F_n^s$  using our measured tacticity data. In Figure 9 we see that the longer sequences are formed only at very low polymerization temperatures. At 12°C, essentially all the sequences are smaller than 14 monomer units, and this is noted in Figure 8 (i.e., about 99.9% of the syndiotactic sequences are less than 14 monomer units long). At 10°C,  $n_{\max}$  is about 16. This suggests that syndiotactic sequence lengths of 14 to 16 monomer units are required for the formation of strong aggregates. The fact that weak aggregates do not form at low temperatures of polymerization leads us to believe that strong aggregate formation involves a nucleation-growth process where the long sequences are nucleation sites. The smaller sequence lengths participate in the growth process. Greater amount of syndiotacticity and longer sequences coupled with longer polymer chains all produced at lower

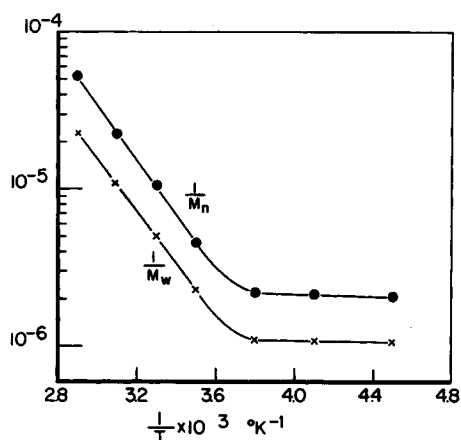


Fig. 10. Effect of polymerization temperature on molecular weight averages

polymerization temperatures create an environment which is suitable for the formation of strong aggregates. The longer polymer chains will contain more and longer syndiotactic sequences.

An examination of Figures 5 and 8 shows that the formation of weak aggregates is much more temperature dependent than that for strong aggregates. The dependence of  $A$  on temperature is similar to that of  $M_n$  and  $M_w$  shown in Figure 10. Numerical values for these molecular weight averages are tabulated in Table II. The range of conversions for these PVC samples was 70–90%. The polydispersity is constant at 2 over the temperature range  $+50^\circ$  to  $-50^\circ\text{C}$ . This is an excellent agreement with our model for the bulk polymerization of vinyl chloride developed in a previous investigation.<sup>13</sup> The molecular weight averages increase as the polymerization temperature falls and reach a plateau at the lower temperatures. This is in disagreement with published data<sup>8,11</sup> where maxima in molecular weight averages were found and where with further reduction in polymerization temperature the averages began to rise. Talamini and Vidotto<sup>11</sup> found the maxima to occur at  $-30^\circ\text{C}$ . They attributed this reduction at yet lower temperatures to be due to the occlusion of radicals in polymer particles with a concomitant reduction in the propagation rate

TABLE II  
Molecular Weight Averages of PVC Made at Different Temperatures

Polymerization temp., $^\circ\text{C}$	$M_n \times 10^{-5}$	$M_w \times 10^{-5}$
70	0.19	0.44
50	0.51	1.03
30	0.94	1.98
12	2.21	4.37
-10	4.61	9.20
-30	4.70	9.41
-50	4.75	9.47

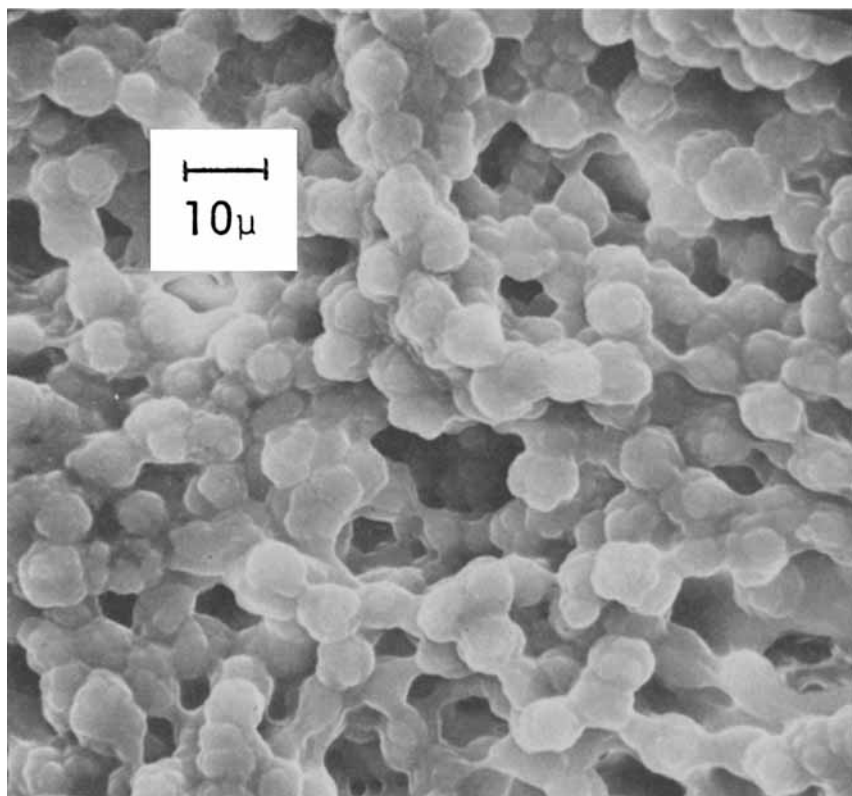


Fig. 11. Electron micrograph of agglomerates of strong aggregates made at  $-50^{\circ}\text{C}$  (scanning electronmicroscope).

constant. Carezza et al.<sup>8</sup> found the maxima to occur at  $-10^{\circ}\text{C}$ . We suspect that these disagreements are most probably due to the elimination of strong aggregates by these investigators<sup>8,11</sup> before their molecular weight measurements. These aggregates are formed preferentially from longer polymer chains, and their elimination by filtration before molecular weight measurement would lead to measured  $M_n$  and  $M_w$  values that are too small. On the basis of our experience, we would recommend the use of our heat treatment procedures before measurement of molecular weight distribution or averages.

## Appendix I

### Aggregate Size Calculation Based on GPC Measurements

The following calculations enable us to obtain a rough estimate of the aggregate size. If  $\bar{r}^2$  is the mean square chain end-to-end distance, then the hydrodynamic volume is related to the molecular weight  $M$  and intrinsic viscosity  $[\eta]$  by the Flory equation,

$$[\eta]M = \Phi(\bar{r}^2)^{3/2}$$

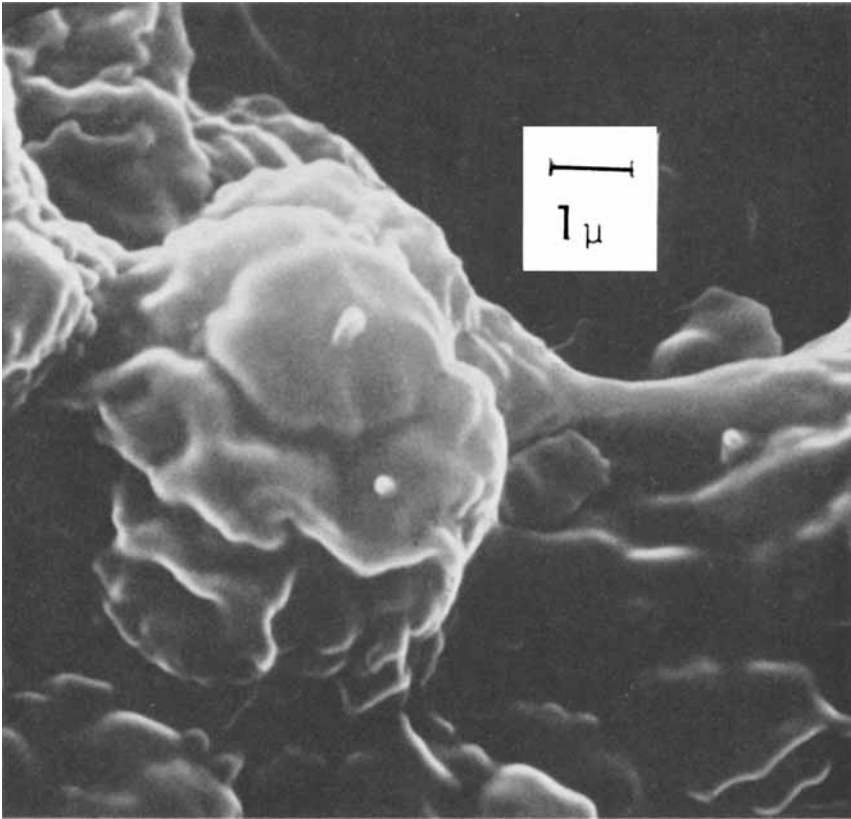


Fig. 12. Enlarged section of Fig. 11.

where  $\Phi$  is the universal Flory's constant  $= 2.5 \times 10^{23} \text{ mole}^{-1}$ . Assuming the aggregate of molecular weight  $M$  to be a sphere of diameter  $D$ , then

$$[\eta]M = \Phi \frac{\Pi}{6} D^3 = f(v)$$

where  $[\eta]M = f(v)$  is the universal calibration curve for GPC. We can therefore relate  $D$  to retention volume as follows:

$$D = \left( \frac{6f(v)}{\Pi\Phi} \right)^{1/3} \text{ \AA},$$

and this modified GPC calibration curve may be used to find the size distribution of the molecular aggregates. It was found that weak and strong aggregates have mass mean sizes of about 2500  $\text{\AA}$  and 4300  $\text{\AA}$ , respectively. Kratochvil et al.,<sup>14,15,16</sup> using light scattering techniques, also estimated the size of PVC aggregates to be of the order of 2500  $\text{\AA}$ . These workers most probably experienced weak aggregates in their measurements.

## Appendix II

### Investigation of Aggregate Geometry by Electron Microscopy

It was of interest to estimate the shape of the size of weak and strong aggregates and to compare the latter with those measured by GPC. Micrographs of PVC samples at

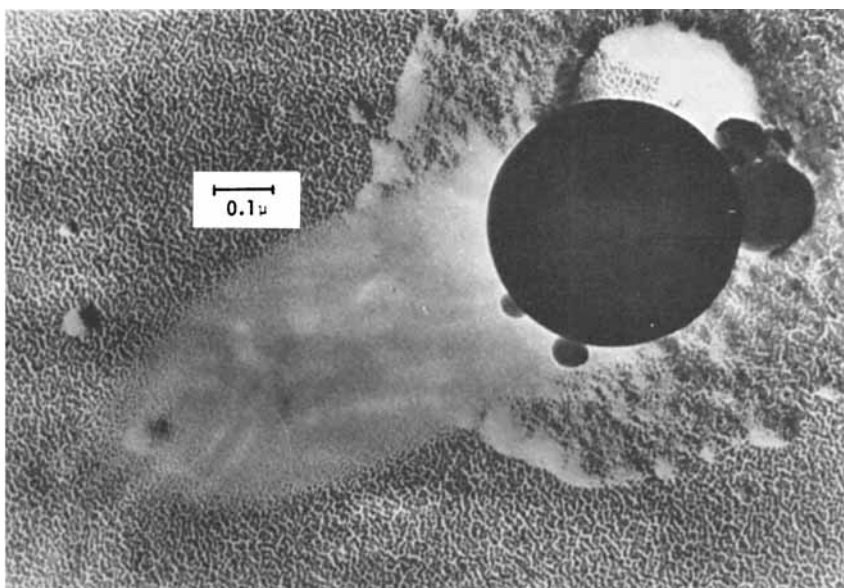


Fig. 13. Electron micrograph of strong aggregates ( $-50^{\circ}\text{C}$ ).

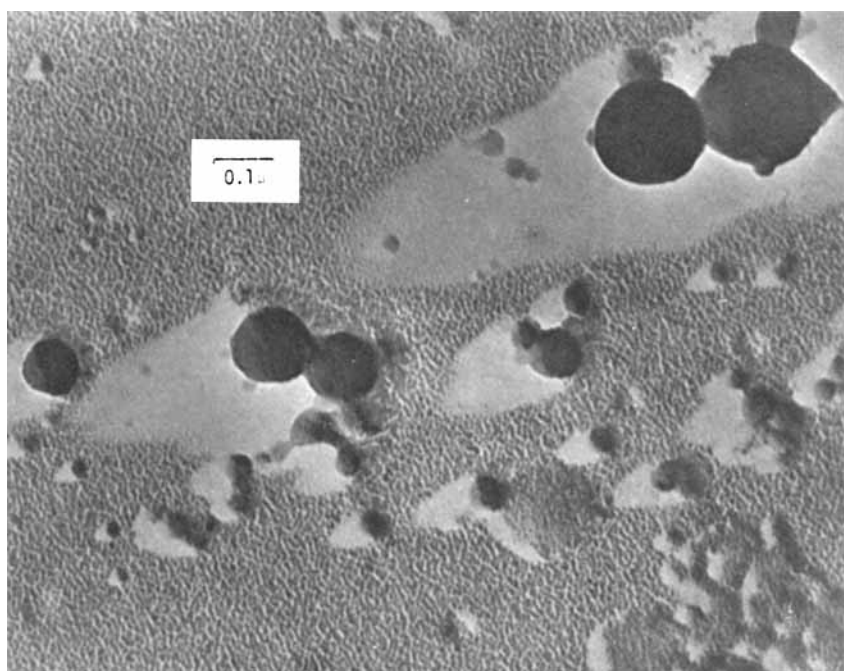


Fig. 14. Electron micrograph of weak aggregates ( $-10^{\circ}\text{C}$ ).

various stages of preparation (see Fig. 1) were made using scanning and transmission electron microscopes.

Figures 11 and 12 show micrographs taken with the scanning electron microscope. This particular PVC was polymerized at  $-50^{\circ}\text{C}$ . The fraction of the polymer in Figures 11 and 12 is undissolved polymer at room temperature collected on 15-micron filter paper. A lump of this dried PVC was placed in a metal base, coated with carbon and palladium, and analyzed with a scanning electron microscope. The micrograph in Figure 11 indicates that the polymer is made up of agglomerates of about 5 microns in diameter connected together by bridges of PVC to form a three-dimensional network. These groups of 5-micron agglomerates would understandably not pass through 15-micron filter paper. Figure 12 shows an enlarged section of Figure 11. The little shiny, white dimples are probably smaller-sized, strong aggregates.

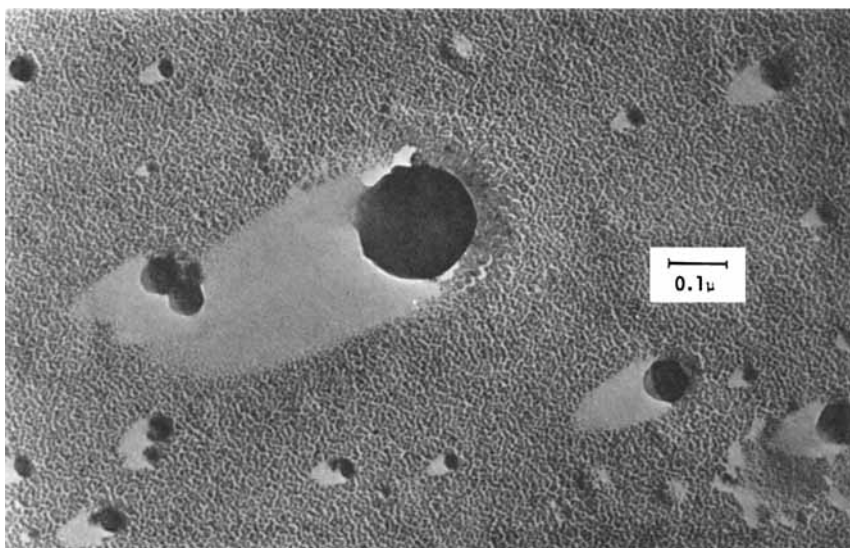


Fig. 15. Electron micrograph of weak aggregates ( $-10^{\circ}\text{C}$ ).

Figure 13 shows a micrograph of a strong aggregate taken with a transmission electron microscope (dark sphere of about  $5000 \text{ \AA}$  in diameter). The smaller spheres are probably smaller, strong aggregates. A solution of strong aggregates ( $-50^{\circ}\text{C}$  PVC in THF at 100 ppm concentration) were sprayed onto Formvar on copper mesh. After a suitable period of THF evaporation, the sample was coated with carbon and palladium. Shadow dimensions indicate that the strong aggregate has an approximately spherical shape with a diameter of about  $5000 \text{ \AA}$ . The weight-average mean diameter of the strong aggregates estimated from GPC measurements was about  $4300 \text{ \AA}$ .

Figures 14 and 15 show micrographs of weak aggregates taken with a transmission electron microscope. Some of the smaller particles shown may be individual PVC molecules. The polymerization temperature of the polymer was  $-10^{\circ}\text{C}$ . A solution of weak aggregates and individual PVC molecules on THF (100 ppm) was used to prepare samples for electron microscopy. Similar spraying and coating procedures were used as with strong aggregates (Fig. 13). The weight-average mean diameter of weak aggregates measured by GPC was about  $2500 \text{ \AA}$ . The larger, weak aggregates in Figures 14 and 15 approach this size.

### References

1. P. Doty, H. Wagner, and S. Singer, *J. Phys. Chem.*, **51**, 32 (1947).
2. J. Lyngaae-Jorgensen, *J. Poly. Sci.*, **C**, 39 (1971).
3. A. Rudin, and I. Benschop-Hendrychova, *J. Appl. Polym. Sci.*, **15**, 2881 (1971).
4. A. H. Abdel-Alim, and A. E. Hamielec, *J. Appl. Poly. Sci.*, **16**, 1093 (1972).
5. J. Lyngaae-Jorgensen, Ph.D. Thesis, The Tech. Univ. of Denmark, 1970.
6. A. Crugnola and F. Danusso, *J. Polym. Sci. B*, **6**(8), 535 (1968).
7. J. Franz, E. Schroder, and K. Thinius, *Plaste Kautschuk*, **18**, 180 (1971).
8. M. Carezza, G. Palma, and M. Tavan, IUPAC, Helsinki, July 2-7, 1972.
9. D. Kockott, *Kolloid-Z.*, **198**, 17 (1964).
10. T. G. Fox, W. E. Goode, S. Gratch, C. M. Huggett, J. F. Kincaid, A. Spell, and J. D. Stroupe, *J. Polym. Sci.*, **31**, 173 (1958).
11. G. Talamini and G. Vidotto, *Makromol. Chem.*, **50**, 129 (1961).
12. W. Kuhn and P. Moser, *Makromol. Chem.*, **44**, 71 (1961).
13. A. H. Abdel-Alim and A. E. Hamielec, *J. Appl. Poly. Sci.*, **16**, 783 (1972).
14. P. Kratochvill, V. Petrus, P. Munk, M. Bohdanecky, and K. Solc, *J. Poly. Sci.*, **C16**, 1257 (1967).
15. P. Kratochvill, *Coll. Czech. Commun.*, **30**, 683 (1965).
16. P. Kratochvill, *Coll. Czech. Commun.*, **29**, 2290 (1964).

Received February 14, 1973